AIAA JOURNAL
Vol. 48, No. 4, April 2010

Aeroacoustics of Drag-Generating Swirling Exhaust Flows

P. N. Shah,* D. Mobed,† and Z. S. Spakovszky‡
Massachusetts Institute of Technology, Cambridge, Massachusetts 02139
and
T. F. Brooks§ and W. M. Humphreys Jr.¶
NASA Langley Research Center, Hampton, Virginia 23681

DOI: 10.2514/1.37249

Aircraft on approach in high-drag, high-lift configurations create inherently noisy flow structures. For flaps, slats, and undercarriage, the strong correlation between overall noise and drag suggests that future quiet aircraft will need to generate drag at low noise levels. This paper presents a novel noise-reduction concept based on the idea that appreciable pressure drag can be generated by a relatively quiet swirling exhaust flow. A first aeroacoustic assessment of ram-pressure-driven swirling exhaust flows and their associated vortex breakdown instability is presented. The technical approach combines 1) an in-depth aerodynamic analysis, 2) qualitative acoustic source descriptions via plausibility arguments, and 3) detailed quantitative phased microphone-array measurements of a model-scale engine nacelle with stationary swirl vanes at a full-scale approach Mach number of 0.17. The analysis shows an acoustic signature composed of 1) quadrupole-type turbulent mixing noise in the swirling core flow and 2) scattering noise from vane boundary layers and turbulent eddies of the burst vortex structure near the nacelle, pylon, and vane centerbody trailing edges. The highest stable swirl-angle setting yields a nacelle-area-based drag coefficient of 0.83 with a full-scale overall sound pressure level of about 40 dBA at the International Civil Aviation Organization approach certification point.

I. Introduction

SWIRLING flows are involved in many fluid machinery applications ranging from combustion chambers, turbomachines and their associated ducting, and cyclone separators. A novel application is based on the concept of exploiting the low pressure in the vortex cores to generate drag. The idea is that a swirling exhaust flow (for example, emanating from an engine nacelle, as shown in Fig. 1) can yield a steady streamwise vortex in which the centripetal acceleration of fluid particles is balanced by a radial pressure gradient. The very low pressure near the vortex core at the exit of the duct generates pressure drag. The aerodynamic analysis of this concept and its practical embodiments are described in detail in Shah [1] and Shah et al. [2]. The simplest possible configuration is a ram-pressure-driven nacelle with a row of stationary swirl vanes (no rotating parts), as depicted in Fig. 1. The stability limit of such a swirling flow is set by vortex breakdown phenomena that are predicted to occur at swirl angles in excess of 50 deg (for an in-depth discussion, see Shah [1] and Greitzer et al. [3]). Aerodynamic wind-tunnel tests of this device were conducted using hot-wire anemometry and flow visualization validating the predicted instability threshold. The device was mounted on a drag balance, and a maximum drag coefficient of 0.83 based on nacelle area was measured, as shown by the curve in Fig. 2. Although high-drag capability is demonstrated, the major unknowns are the acoustic signature of such swirling flowfields and the impact of vortex breakdown on the noise levels. It is important to note that the flow investigated here is markedly different from a swirling jet. Because the flow is not pumped to a higher total pressure than the ambient air, the ram-air-driven nacelle with swirl vanes sets up a wakelike flow with a streamwise vortex. The acoustic assessment of such drag-generating swirling exhaust flows has not yet been reported and is the focus of this paper.

Related previous work is that of acoustic sources in circular motion and noise from swirling jets. Tanna and Morfey [4] evaluated the sound radiated in the far field due to point sources of random time variation rotating uniformly in a circle at subsonic speed. This approach was extended by Tanna [5] to assess the effect of swirling motion of sources on subsonic jet noise. The directivity change due to swirling motion was found to be a strong function of tangential Mach number, with a maximum effect at 90 deg to the jet axis. Since the on-axis radiation from a randomly oriented point quadrupole moving uniformly on a helical path is independent of swirl and controlled by the axial velocity component, the magnitude of the offaxis radiation with swirl increases with swirl angle.

Jet-noise suppression by swirling the jet flow was stimulated by Schwartz [6], who obtained a ratio of 3 dB overall sound power reduction to 1% of thrust loss for a Pratt & Whitney JT15D-1 bypass flow engine by swirling a part of the primary flow. Schwartz's swirl vanes spanned an outer annular section of the engine's afterburner and allowed a core flow to pass without swirl. Since the measured JT15D-1 engine noise contained jet noise, core noise, and noise sources due to swirl, Lu et al. [7] measured the noise and flow characteristics of isolated model-scale swirling jets. The authors report that swirling-jet noise is broadband in nature, similar to nonswirling-jet noise, with noise attenuation due to swirl at angles less than 40 deg from the jet axis and noise increase at side directivity angles. The difference between swirling- and nonswirling-jet noise levels increases with swirl angle and decreases with increasing pressure ratio and total temperature. It was found that the largest noise increases due to swirl occurred in cases in which a plug nozzle allowed high-velocity centerline flows to occur; this effect was significantly suppressed by permitting a nonswirling core flow (similar to Schwartz's case). It was concluded that considerable further testing of swirling-jet flow and noise, especially under the influence of a parallel mean flow, is required to advance the understanding of the acoustic signature of such exhaust flows.

The present paper focuses on the novel idea of swirling an exhaust flow for the express purpose of quiet drag generation on aircraft,

Presented as Paper 3714 at the 13th AIAA/CEAS Aeroacoustics Conference, Rome, Italy, 21–23 May 2007; received 3 May 2008; revision received 17 March 2009; accepted for publication 19 April 2009.

*Ph.D. Student, Department of Aeronautics and Astronautics, Gas Turbine Laboratory, 77 Massachusetts Avenue. Member AIAA.
†M.S. Student, Department of Aeronautics and Astronautics, Gas Turbine Laboratory, 77 Massachusetts Avenue. Member AIAA.
‡Associate Professor, Department of Aeronautics and Astronautics, Gas Turbine Laboratory, 77 Massachusetts Avenue. Member AIAA.
§Senior Research Scientist, Aeroacoustics Branch. Fellow AIAA.
¶Senior Research Scientist, Aeroacoustics Branch. Senior Member AIAA.

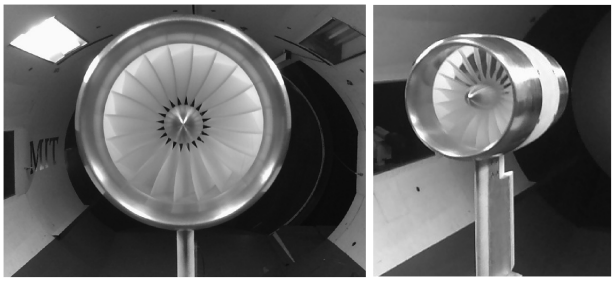

Fig. 1 Aerodynamic flow testing and drag measurements of swirling exhaust flows [1,2].

differentiating the work from past research on noise from swirling jets. Specifically, the design of a swirling outflow device that maximizes drag with minimal noise penalty is uniquely motivated by the need to enable the quiet approach of an aircraft in a high-drag, high-lift configuration.

The objectives of this paper are as follows:

1) Quantify the noise levels of drag-generating swirling exhaust flows.

2) Identify noise mechanisms and dissect source locations in such flows.

3) Establish scaling laws and the relation between swirl, drag, and radiated sound power.

The working hypothesis is that the acoustic signature is composed of quadrupole-type turbulent mixing noise of the swirling core flow and scattering noise from vane boundary layers and turbulent eddies of the burst vortex structure by sharp edges such as the exposed trailing edge of the nacelle, centerbody, and pylon.

The paper is organized as follows. First, an overview of the relevant aerodynamic flow features of the investigated swirling exhaust flows is given. Next, plausibility arguments for the qualitative assessment of the acoustic sources are followed by the design of acoustic experiments. Then the measured far-field spectra are analyzed and key acoustic features are identified. Using the deconvolution approach for mapping of acoustic sources (DAMAS), array-data processing-noise source maps are established and are used to investigate the noise-generation mechanisms. The source noise in different regions of the flowfield is quantified. Both stable swirling flows and swirling flows with vortex breakdown are considered. then scaling laws are established using the source noise maps, corroborating the hypotheses and qualitative assessments. Last, the work is summarized and concluding remarks are given.

II. Aerodynamic Features of Swirling Exhaust Flows

The aerodynamic design and analysis of the ram-pressure-driven nacelle with stationary swirl vanes is discussed in detail in Shah et al. [2] and only the relevant features of the swirling flow are briefly summarized here. The vanes are designed to yield a Burger vortex-type circulation distribution approaching forced vortex flow in the core and free-vortex-type behavior on the outer periphery. A model-scale engine nacelle with stationary swirl vanes of 0.179 m outer diameter was built and tested in the Massachusetts Institute of Technology's Wright Brothers Wind Tunnel. The vanes are integral to a disk that can be exchanged to achieve various angles. Vane angles of 0, 34, 41, 47, 53, 57, and 64 deg were implemented and experimentally tested using hot-wire anemometry and flow visualization. Figure 3 shows a comparison between the predicted axial and tangential velocity profiles using three-dimensional steady Reynolds-averaged Navier–Stokes (RANS) calculations (marked by pluses) and hot-wire traverse measurements (marked by circles) for the nacelle with a swirl-vane-angle setting of 47 deg. The results indicate good agreement between the predictions and the experiment, validating the swirl-vane design. Note that there is a region of increased axial velocity and high shear near the core region and a deficit in axial velocity, leading to a wakelike structure on the outer periphery. The excess in centerline axial velocity is correlated with both the swirl-angle setting and the centerline pressure deficit.

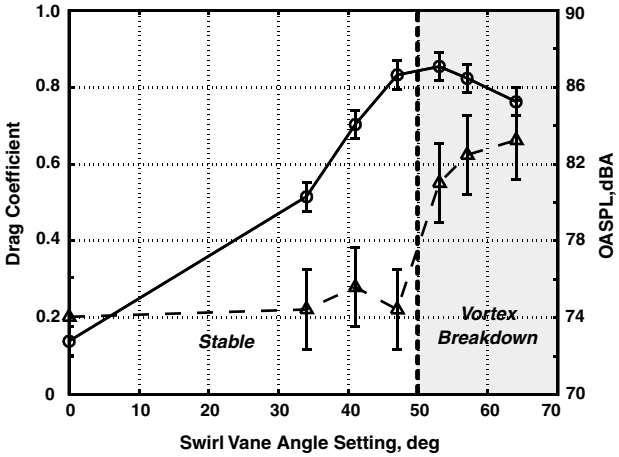

Fig. 2 Experimentally measured drag coefficient (solid line) and overall sound pressure level at a polar angle of 90 deg and 1.5 m distance (dashed line) for swirling exhaust flows [1,2].

The swirl-vane-angle setting of 47 deg yields an experimentally measured drag coefficient of 0.83, the highest drag coefficient without vortex breakdown. The predicted drag coefficient of 0.8 falls well within the measurement uncertainty of ± 0.04. The limiting phenomenon for stable flow is vortex breakdown, which is associated with the rapid expansion of the core when a critical swirl-angle distribution is reached [1–3]. For the Burger vortex distribution implemented here, vortex breakdown was measured to occur for vane angles greater than 50 deg, in good agreement with the theory and simulations. A separation bubble forms downstream of the nacelle and creates blockage and high levels of turbulence, reducing the drag-generation capability and dramatically increasing the noise level, as shown in Fig. 2. The mechanism of noise generation is the focus of this paper and is discussed next in depth.

III. Qualitative Description and Plausibility Arguments for Acoustic Sources

It is hypothesized that the acoustic signature is composed of quadrupole-type turbulent mixing noise of the swirling core flow and scattering noise from vane boundary layers and turbulent eddies of the burst vortex structure near sharp edges exposed to the flow. In what follows, a qualitative description and plausibility arguments for the acoustic sources are given in support of the experimental noise-source measurements. In particular, steady axisymmetric RANS simulations of the swirling exhaust flow are coupled with a preliminary acoustic analysis based on the fine-scale-turbulence jet noise model by Tam and Auriault [8] and the description for swirling sources by Tanna [5]. Scaling laws for scattering of aerodynamic sound by sharp edges based on Lighthill's acoustic analogy and using the reciprocal theorem [9,10] are employed to support the hypothesis that scattering noise may play an important role in the noise generation. These arguments are based on a simplified analysis such that experiments are necessary to determine the relative influence of the scattering and the quadrupole-type sources.

In the absence of a rigorous theoretical framework to predict the quadrupole noise from a swirling flow it is assumed that the source strength between helically and axially convected sources is unchanged. The fine-scale-turbulence mixing noise of the swirling flow at a polar angle of 90 deg is estimated from steady axisymmetric RANS calculations in combination with Tam and Auriault's [8] semi-empirical expression for the spectral density S of straight jets:

$$S(\mathbf{x},\omega) = 4\pi\left(\frac{\pi}{\ell_n 2}\right)^{3/2} \cdot \iiint_{\mathrm{Vol}} \frac{\hat{q}_s^2 l_s^3}{c_o^2 \tau_s} \frac{\exp\left[\frac{\omega^2 l_s^2}{\bar{u}^2(4\ell_n 2)}\right]}{\left[1+\omega^2\tau_s^2\left(1-\frac{\bar{u}}{a_\infty}\cos\theta\right)^2\right]} |p_a(\mathbf{x}_2,\mathbf{x},\omega)| \mathrm{d}\mathbf{x}_2 \quad (1)$$

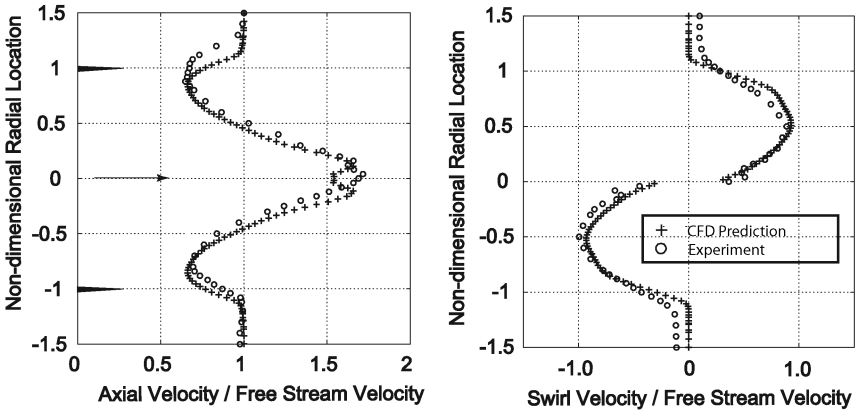

Fig. 3 Experimental validation of predicted axial and tangential velocity profiles at two diameters downstream of nacelle for swirl-vane setting of 47 deg; CFD prediction (+) and hot-wire measurements (○).

In the above expression, the averaged turbulence kinetic energy k and dissipation rate ε from the simulation are used in combination with the empirically defined constants of Tam and Auriault [8]** to set the turbulence decay time τ_s, length scale l_s, and the rms of the fluctuating kinetic energy of the fine-scale turbulence $\hat{q}_s$. The spectral density integrand is further modified by a noise-amplification factor for the helical motion of sources given by Tanna [5]:

$$\frac{\langle p'^2\rangle_{\text{Helical}}}{\langle p'^2\rangle_{M_\theta=0}} = F_1(\alpha') + \left(\frac{\Omega}{\nu}\right)^2 F_2(\alpha') + \left(\frac{\Omega}{\nu}\right)^4 F_3(\alpha') \qquad (2)$$

with

$$\alpha' = \frac{M_\theta \sin\psi}{1 - M_\theta \sin\psi} \qquad (3)$$

where ν is the source radian frequency; Ω is the rotation radian frequency; F_1, F_2. and F_3 are functions; and α' is defined in terms of the observer angle ψ and the axial and tangential Mach numbers of the swirling flow. The one-third-band sound pressure spectrum may then be written as

$$\text{SPL}\,(f) = 10\log\left[\frac{\langle p'^2\rangle_{\text{Helical}}}{\langle p'^2\rangle_{M_\theta=0}}\frac{4\pi S(\mathbf{x},\omega)}{p_{\text{ref}}^2}\right] + 10\log(\Delta f_{\text{Hz}}) \qquad (4)$$

In the limit of zero swirl angle, a straight jet or wake flow is recovered. The developed methodology was validated against jet noise data available in literature. The methodology was subsequently used to estimate the fine-scale-turbulence mixing noise of the swirling exhaust flows under consideration. Figure 4 shows the predicted one-third-octave frequency spectra for vane angles of 34 and 47 deg together with the measured background noise spectrum of the NASA Langley (LaRC) Quiet Flow Facility (QFF). The bottom of Fig. 4 also shows the distribution of the spectral density integrand of Eq. (1) near the peak one-third-octave frequency. The results indicate that the estimated noise sources seem to be concentrated in the shear layer and near the core of the swirling flow. The fine-scale-turbulence mixing noise is rather quiet as compared to the background noise. The qualitative assessment suggests the following:

1) Other noise sources that are stronger radiators than the quadrupoles of the turbulence mixing noise might be at play and need to be captured.

2) Swirling-flow turbulence mixing noise increases with the level of swirl.

3) From a measurement perspective, phased microphone-array methods together with advanced source-mapping algorithms need to be employed to dissect the noise-generation mechanisms.

**It has been shown [9] that under consistent assumptions, the model of Tam and Auriault [8] and Lighthill's acoustic analogy models can yield very similar noise predictions; here it is used to qualitatively estimate the nature of the turbulence generated swirling-flow noise due to its good agreement with experiments for straight jets.

It will be shown that quadrupole-type turbulence mixing noise is dominant at high Strouhal number, and scattering-type noise sources are apparent at intermediate Strouhal numbers. Given the limitations of the above computational approach, an improved noise-estimation method for swirling exhaust flows needs to be developed in future work.

The scattering of aerodynamic sound by a sharp edge such as the trailing edge of the nacelle, the centerbody, or the pylon can be described using Lighthill's acoustic analogy and by applying the reciprocal theorem [9,10]. The scaling of the amplitude of density perturbations generated by turbulent quadrupoles near a scattering surface can be expressed as

$$\langle \rho'^2\rangle \propto \rho_o^2 M^5 \left(\frac{l}{y}\right)^3 \frac{l^2}{r^2}\sin^2\left(\frac{1}{2}\theta\right) \qquad (5)$$

where l is the length scale of the turbulent eddy located at a distance y from the edge. At low Mach numbers the generated scattering sound is more than the free space sound of the same eddy by a factor $M^{-3}l^3/y^3$. Scattering surfaces dominate the source structure of low Mach number flows and it will be shown that the acoustic signature of drag-generating swirling exhaust flows is governed by the combination of scattering noise from vane boundary layers by sharp edges and quadrupole-type turbulent mixing noise in the vortex core. The main difference between a stably swirling flow and a flow with vortex breakdown is that the former yields distinct spatial separation of the two source mechanisms, whereas the noise sources of the latter

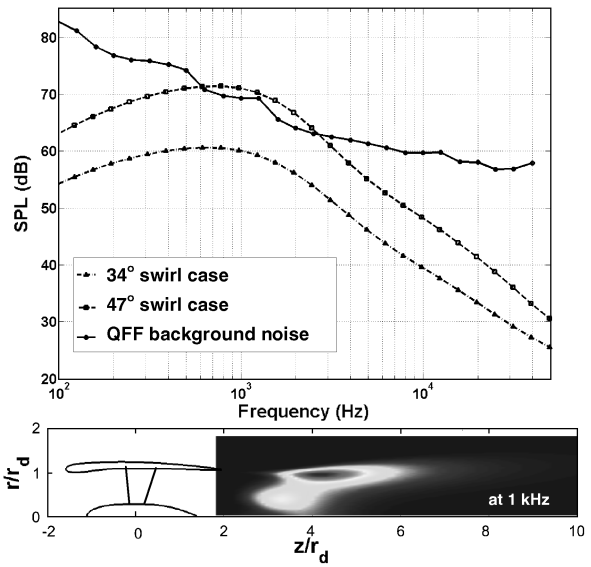

Fig. 4 Predicted fine-scale-turbulence noise of swirling exhaust flows at a polar angle of 90 deg and distribution of spectral density integrand.

are concentrated near the nacelle exit. The increased noise levels for vortex breakdown, as shown in Fig. 2, are due to the combined effect of a reduced distance between the eddies of the burst vortex structure and the solid edges and an increase in the turbulence intensity and the spatial extent thereof.

IV. Design of Experiments and Acoustic Testing

The scale-model nacelle with various swirl-vane-setting angles was tested in the NASA LaRC QFF. The facility has been used in measurements of airfoil self-noise [11], distributed trailing-edge noise [12], flap-side edge noise [13], and leading-edge slat noise [14]. The 9.1 by 6.1 by 7.6 m anechoic test chamber has a vertically flowing 0.6 by 0.9 m free jet exhausting through the ceiling. Free-jet Mach numbers of up to 0.17 can be achieved. A total of six fixed-pole microphones are located on either side of the free jet and a medium-aperture directional array (MADA) consisting of 41 microphones is mounted on a boom that can rotate on a polar arc, as shown in Fig. 5 on the left. The nacelle was mounted on a pylon with a NACA 0022 profile that was attached to one of the two side plates of the wind tunnel. The model size was chosen such that, given the spatial test window, the swirling exhaust flow stayed well within the potential core of the free jet. To ensure that the noise signature is not affected by possible interactions between the shear layer of the free jet and the swirling exhaust flow, the nacelle was mounted at different axial locations. Noise measurements showed that the acoustic signature was insensitive to the nacelle location. The boundary layers of the pylon, the nacelle, and the swirl vanes were tripped to ensure turbulent flow. The pylon trailing edge was serrated to mitigate trailing-edge noise that could contaminate the swirling-exhaust-flow noise measurements.

The experimental test matrix was composed of pylon-only measurements; empty-nacelle tests; and measurements with vane angles of 0, 34, 41, 47, 53, 57, and 64 deg, ranging from zero swirl to highly swirling flow with vortex breakdown. In addition, tests were conducted with positive and negative nacelle angles of attack and various upstream flow nonuniformities. This included a blade wake generator simulating an upstream blade row and perforated plates of 120 deg circumferential extent modeling inlet flow distortion, common in engine inlets. In Secs. V and VI of this paper, results are shown for different swirl-vane angles, with the nacelle oriented at a 0 deg angle of attack and having clean inlet airflow. Details of the additional test cases including angle-of-attack variation and inlet distortion may be found in Mobed [15].

The DAMAS technique developed by Brooks and Humphreys [16,17] was employed to map the noise sources of the drag-generating swirling exhaust flows. In previous research, the technique was successfully applied to distributed sources near solid bodies such as wing trailing edges, leading-edge slats, or flap-side edges. This is the first time that the DAMAS technique is applied to measure quadrupole-type volume sources.

V. Swirling-Exhaust-Flow Sound Pressure Spectra

To help identify scaling laws and directivity, microphone-array data were acquired at wind-tunnel Mach numbers of 0.07, 0.09, 0.11, 0.13, 0.15, and 0.17 and at various MADA array angles, as depicted in Fig. 6. Two forward angles at −124 and −107 deg; the sideline angle at −90 deg; and three aft angles at −73, −56, and −45 deg were investigated. Results in this paper are presented for the −90 deg MADA angle only.

Figure 7 illustrates the acoustic features of various swirling exhaust flows together with the sound pressure spectra of the wind tunnel only and the empty nacelle (no swirl vanes). Autospectra with constant bandwidth of 17.44 Hz at a polar angle of −90 deg and an observer distance of 1.5 m are plotted for a wind-tunnel Mach number of 0.17. All spectra are primarily broadband in nature, with good signal-to-noise ratio for frequencies above 1 kHz.

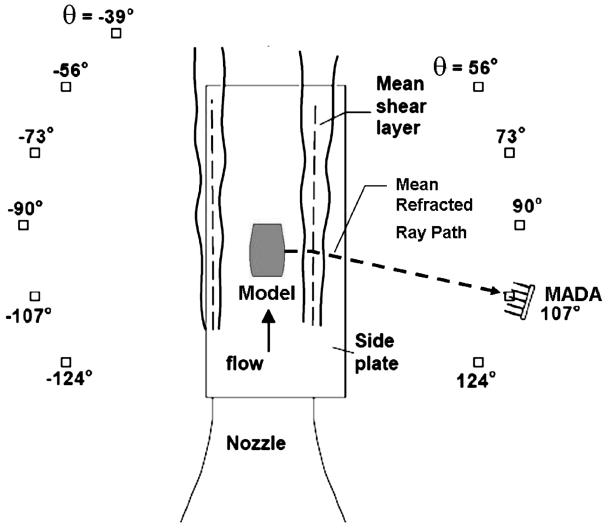

Fig. 6 Data were acquired at standard MADA array angles from −124 to −45 deg. Results in Secs. V and VI are shown for −90 deg MADA angle.

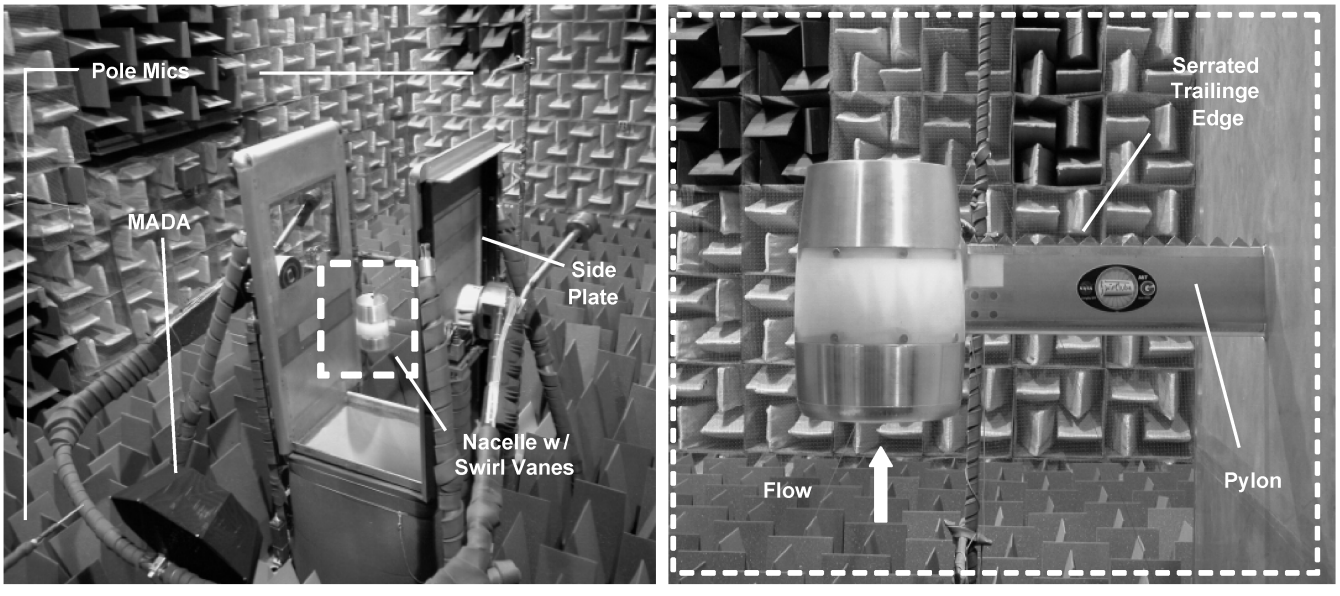

Fig. 5 Scale-model nacelle with swirl vanes mounted in the QFF test facility at NASA LaRC.

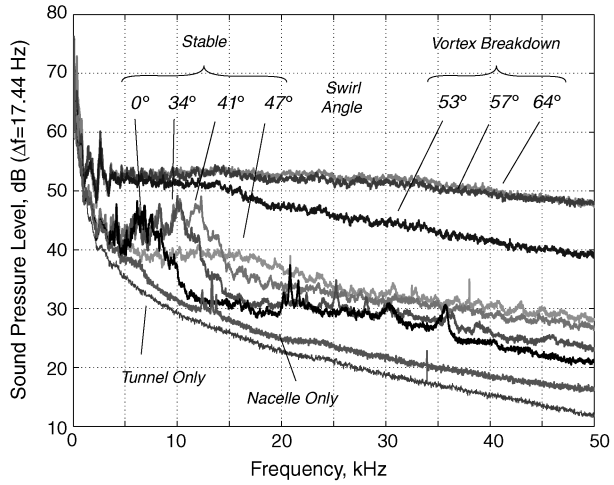

Fig. 7 Narrowband ($\Delta f = 17.44$ Hz) sound pressure spectra for swirling exhaust flows at $M = 0.17$, polar angle −90 deg and 1.5 m distance.

Trailing-edge noise due to the scattering of turbulent-boundary-layer structures is observed in the 2–3 kHz range for the pylon-only and nacelle-only cases. It will be shown in the next section that the sound pressure levels scale with the freestream Mach number to a power between 5 and 5.5, consistent with classic airfoil self-noise measurements [11].

The sound pressure spectra of swirling exhaust flows may be characterized by two types: 1) stable swirling flows with broadband peaks in the lower frequency range (vane angles of 0 to 47 deg) and 2) flows with vortex breakdown (vane angles 53 to 64 deg) exhibiting white-noise-like spectra dramatically louder than their stable counterparts. The broadening of the low-frequency peak in the 47 deg vane-angle-setting case suggests transition from stable exit flow to vortex breakdown, conjectured to be due to the onset of standing wave patterns on the vortex core (for details, see Shah et al. [2]).

Comparison of the nacelle-only case with the stable swirling-flow cases (0 through 47 deg vane-angle setting) suggests that the presence of the swirl vanes gives rise to low-frequency broadband peaks seen in the 5–20 kHz range. The spectra roll off at higher frequencies and the noise levels and peak frequencies increase with swirl-angle setting. The observations lead to the following hypotheses:

1) The broadband spectral peaks of the stable swirling-flow cases are suggested to be due to the scattering noise of vane boundary layers governed by the swirling-exhaust-flow Mach number.

2) The higher-frequency noise is predominantly due to quadrupole-type mixing noise of the swirling exhaust flow.

3) The vortex breakdown spectra are dominated by scattering noise of the turbulent eddies of the burst vortex structure near sharp edges and turbulent-flow mixing noise, suggesting a Mach number scaling power between five and eight.

These hypotheses are assessed in detail next. The overall noise signature is dissected into zonal spectra using DAMAS postprocessing, and Mach number scaling laws are extracted to determine the fundamental noise mechanisms. Assuming that the swirling-flow Mach number is found to be the governing parameter for scattering-type noise at a fixed swirl-angle setting, the nacelle exit zonal spectra at different freestream Mach numbers should collapse to a single spectrum using a power law for the sound pressure level and peak frequency scaling based on Strouhal number. A similar approach is taken to assess quardupole-type turbulent mixing noise and vortex breakdown noise.

VI. Dissection of Noise Sources and Scaling Laws

Two specific high-drag cases (see Fig. 2), one for stably swirling flow and the other for vortex breakdown, are first discussed in detail to demonstrate the dissection of noise sources using DAMAS postprocessing. Next, the scaling laws are established using the entire test matrix.

The nacelle with a swirl-vane-angle setting of 47 deg was tested at various polar angles and Mach numbers. This swirl case exhibits stable flow, as discussed earlier and illustrated by flow visualization in Fig. 8. Helical motion of fluid particles is observed, and turbulent diffusion and mixing of the swirling exhaust flow occurs downstream of the nacelle. Model-scale one-third-octave-band autospectra of two array microphones are also plotted in Fig. 8 marked by the uppermost curves for a tunnel Mach number of 0.17 and a microphone-array angle of −90 deg (sideline position similar to the one indicated on the left side of Fig. 6). The QFF empty-tunnel background noise is marked by the thin line indicating that data is acquired with a high signal-to-noise ratio for frequencies greater than 1 kHz. The swirling-flow spectra are broadband, with important noise-source features near 2.5 and 16 kHz (indicated by the arrows) that are shown in DAMAS maps in the next subsection.

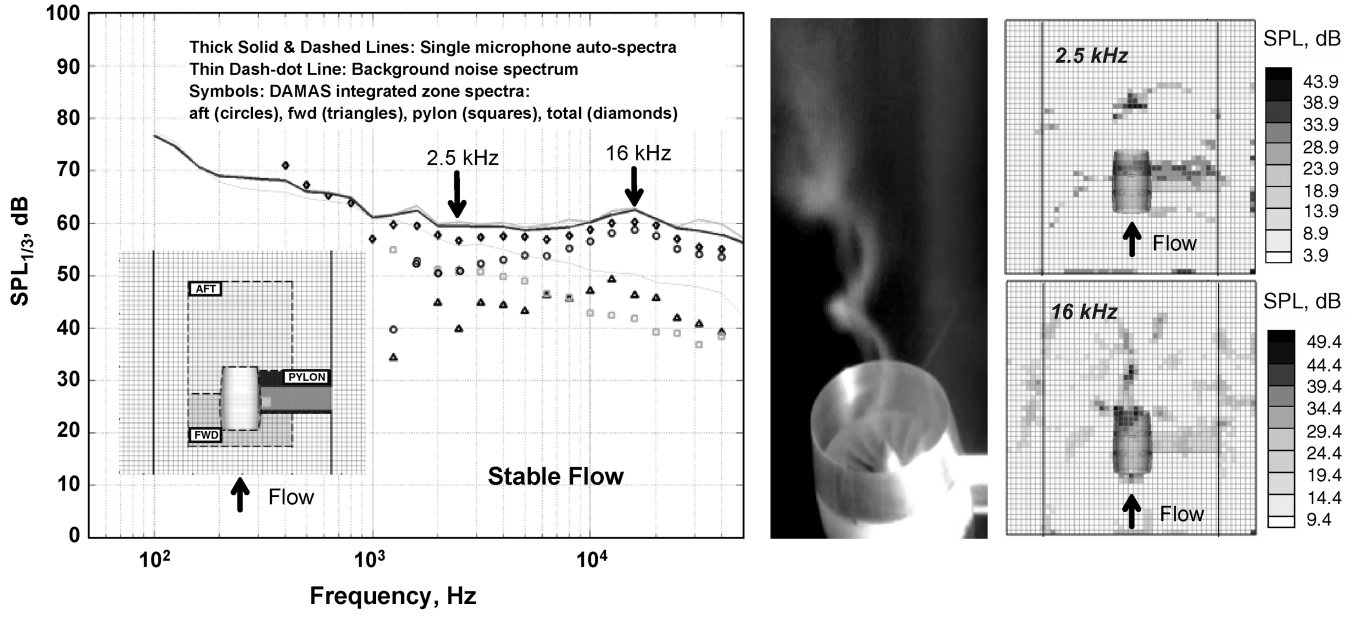

Fig. 8 One-third-octave-band spectra and DAMAS source maps for swirl-vane-angle setting of 47 deg. Zonally integrated spectra shown are aft (circles), forward (triangles), pylon (squares), and total (diamonds).

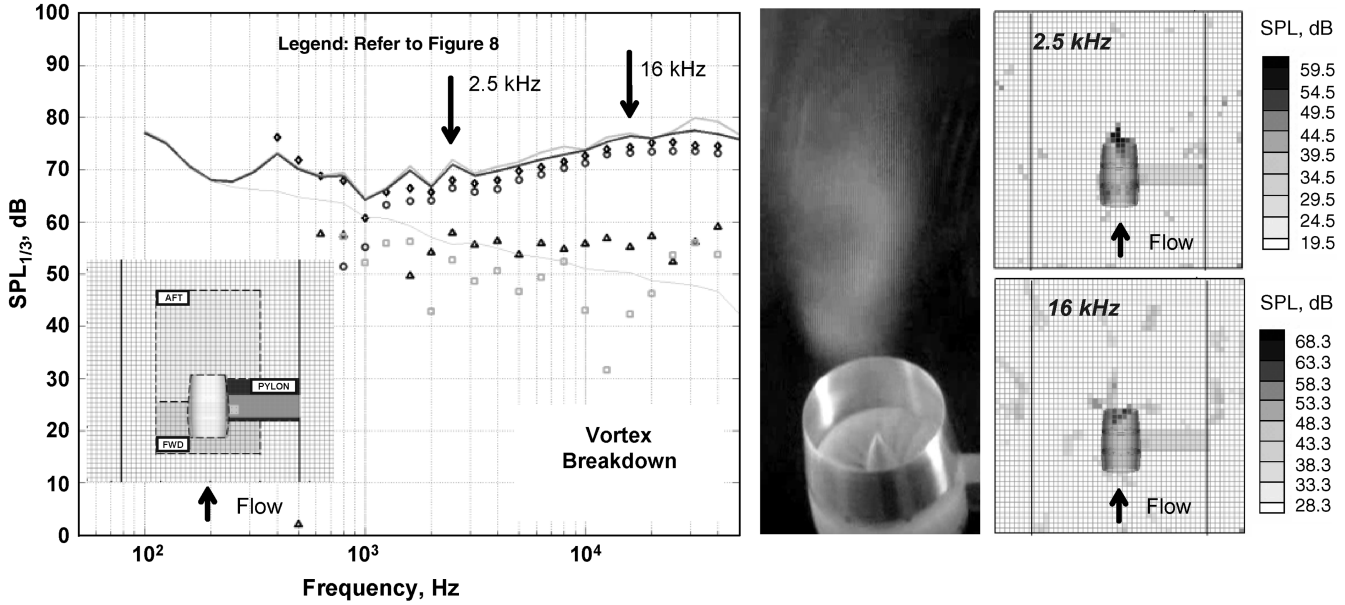

Fig. 9 One-third-octave-band spectra and DAMAS source maps for swirl-vane-angle setting of 57 deg. Zonally integrated spectra shown are aft (circles), forward (triangles), pylon (squares), and total (diamonds).

A. DAMAS Noise Source Mapping and Zonal Spectra

DAMAS postprocessing allows the spatial mapping of sources. For any given frequency, the total sound pressure level of a zone on the scanning grid can be obtained by simply summing the mean square value of the pressure fluctuations of the grid points of interest. In Fig. 8, the following three zones are defined: the top zone is the aft region enclosing the swirling flow and the nacelle exit, the bottom zone is the forward region enclosing the nacelle inlet, and the rightmost zone is the pylon region containing the pylon leading and trailing edges. To assess this procedure, the three zones are summed up at each of the one-third-band frequencies (diamonds) and compared against the single-microphone autospectra. Good agreement is achieved validating the zonal mapping procedure. Note that the sum of the zonal spectra is slightly below the single-microphone autospectra, since the former is limited to the zones only and thus does not contain all the noise sources in the field.

Using the same shading code, each individual zonal spectrum is also shown in Fig. 8. The results indicate that the pylon noise (squares) is well below the background noise and most dominant in the 1 to 3 kHz range. This is in agreement with the source noise map at 2.5 kHz, shown on the top right. The noise radiated from sources in the forward zone is at much lower sound pressure levels, as seen by the triangles. Sound from the aft zone (circles) dominates the acoustic signature for frequencies greater than 3 kHz. Per the source maps on the right of the figure, there are volume sources downstream of the nacelle trailing edge in the vortex core visible in the source noise maps at 2.5 and 16 kHz.

As discussed in the next subsection, the Mach number scaling of the frequency spectra shows that the very-high-frequency noise is of quadrupole type. Scattering noise near the nacelle trailing edge and centerbody is also observed. It will be shown that the sound pressure level scales with the Mach number close to a power of 6.5, corroborating the hypothesis that this noise-generation mechanism is present and different from classical trailing-edge scattering noise, due to the effect of swirl.

Figure 9 depicts similar plots for a swirl-vane-angle setting of 57 deg for which vortex breakdown occurs. The flow visualization illustrates bubble-type vortex breakdown [2] near the nacelle trailing edge. The frequency spectrum indicates dominant acoustic activity in the aft region for all selected frequency bands. An increase in noise levels of 10 to 15 dB as compared to the stable flow case shown in Fig. 8 is observed. The source noise maps corroborate the hypothesis that scattering noise from the nacelle and centerbody trailing edge and turbulent mixing noise dominate the acoustic signature.

B. Scaling Laws for Swirling-Exhaust-Flow Noise

To further assess the nature of the noise sources, Strouhal-number- and Mach-number-based scaling of zonal spectra is carried out using the measurements at different tunnel velocities and different vane angles. The spectra of the stable swirling-flow cases are found to scale differently at low and high frequencies, indicating that multiple noise-source mechanisms are at play. For a given swirl-vane-angle setting, the characteristic Mach number is found to be the freestream Mach number. The vortex breakdown cases exhibit a markedly different acoustic signature and appear to scale according to a combination of scattering and quadrupole-type sources concentrated near the nacelle exit.

The first step in the dissection of the noise sources is the scaling of zonal spectra. In general, the entire region aft of the swirl-tube nacelle exit was found to be the major contributor to the overall noise signature. This region was then further divided into the two subdomains shown in Fig. 10, the nacelle exit domain encompassing regions close to the nacelle trailing edge and the swirling outflow domain encompassing regions downstream of the exhaust plane.

Table 1 summarizes the experimentally determined power-law exponents using Mach number scaling of DAMAS integrated zonal spectra of the different test articles. The following conclusions may

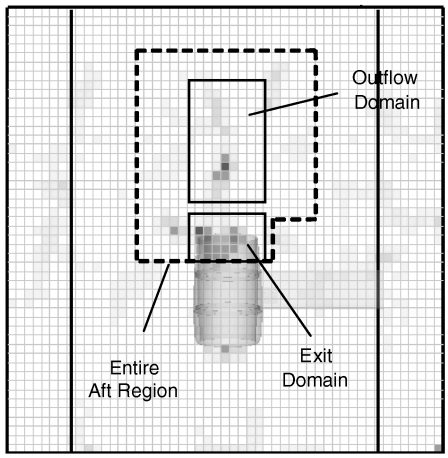

Fig. 10 Definition of subdomains near the nacelle exit for DAMAS-based identification of noise-source mechanisms.

Table 1 Mach-number-based power-law exponents for zonal spectra defined in Fig. 10

Swirl-vane-angle setting	Deduced power-law n		
	Exit domain	Outflow domain	Entire aft region
Empty nacelle	5–5.5	——	——
0 deg	5–5.5	——	——
34 deg	~6.5	~8.0	——
41 deg	~6.5	~8.0	——
47 deg	~6.5	~8.0	——
53 deg	——	——	7.5
57 deg	——	——	7.5
64 deg	——	——	7.5

be drawn from the table regarding the nature of the noise sources. To begin, we consider the working hypothesis that the sound generated near the nacelle exit is primarily due to vane and nacelle trailing-edge scattering noise. The deduced Mach number exponent of 5 to 5.5 in the empty nacelle and no swirl (0 deg swirl-vane-angle setting) suggests that the DAMAS system is well calibrated to detect airfoil self-noise-type sources. Figure 11 depicts the spectra for a swirl-vane setting of 0 deg at various Mach numbers, scaled at a power of 5.5. The Strouhal number is based on nacelle diameter and freestream velocity.

1. Stable Swirling-Flow Noise

The zonal spectra for all vane angles that yield stable swirling flow were analyzed and only the case for a swirl-angle setting of 47 deg is discussed here. The results are summarized in Table 1 and suggest that the noise sources are composed of two distinct mechanisms present in the two subdomains of the nacelle aft region. Near the nacelle exit, the zonal spectra scale with Mach to the power of 6.5, as depicted in Fig. 12 for a swirl-vane-angle setting of 47 deg. The broadband frequency peaks identified earlier in Fig. 7 correspond to a Strouhal number of 48 and are conjectured to be due to scattering and dipole-type noise sources, as shown by the DAMAS source noise map in Fig. 12. While scattering and dipole-type noise effects are present near the exit of the nacelle, the analysis together with the plausibility arguments given earlier suggest that the swirling outflow domain is dominated by quadrupole-type turbulent mixing noise. In Fig. 13, the one-third-octave band spectra are scaled with the eighth power of freestream Mach number supporting the hypothesis. It is worth noting that these experiments constitute the first application of the DAMAS postprocessing technique to volume sources, successfully demonstrating the identification of quadrupole sources and making the procedure also viable for jet noise diagnostics.

2. Vortex Breakdown Noise

The vortex breakdown noise was audibly louder, resembling white noise with a cracklelike sound compared to the hisslike noise of the stable swirling cases. As illustrated by the flow visualizations presented earlier in the paper, swirl-angle settings in excess of 47 deg yield classic bubble-type vortex breakdown [18,19] near the nacelle trailing edge, with dominant acoustic activity in the aft region for all frequency bands. Noise appears to be intensified by the turbulence of the burst vortex structure scattered near the nacelle and centerbody trailing edges. Similar Mach number scaling performed on the zonal spectra for swirl angles of 53, 57, and 64 deg shows excellent

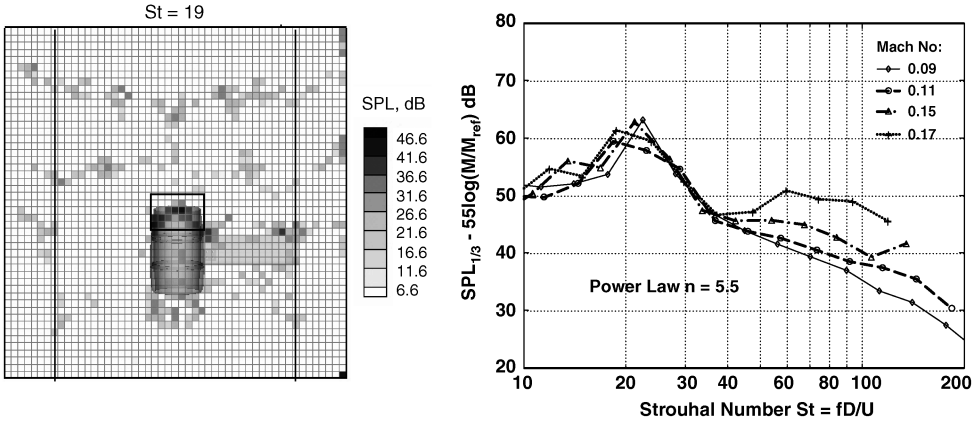

Fig. 11 Exit-domain-based one-third-octave-band spectra scaled with Mach number to power 5.5 for 0 deg swirl-vane-angle setting (no swirl); DAMAS source noise map at $St = 19$.

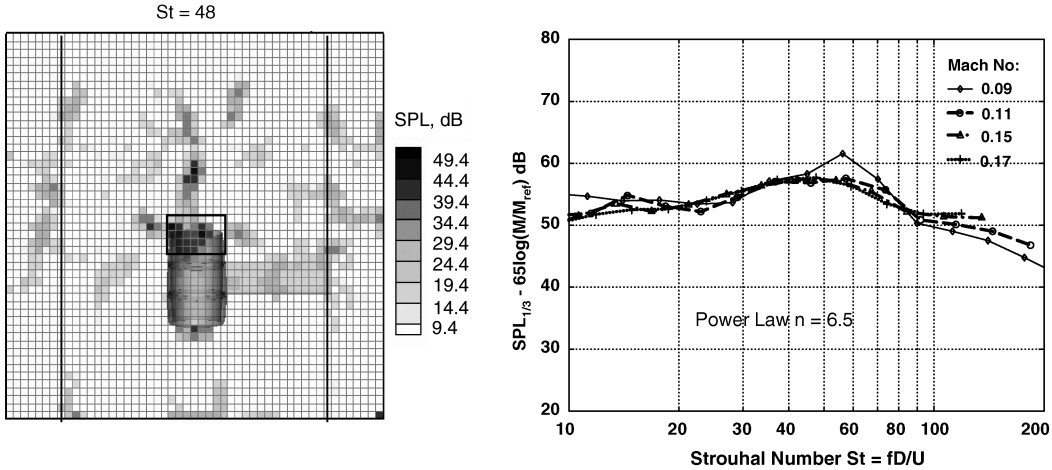

Fig. 12 Exit-domain-based one-third-octave-band spectra scaled with Mach number to power 6.5 for 47 deg swirl-vane-angle setting; DAMAS source noise map at $St = 48$.

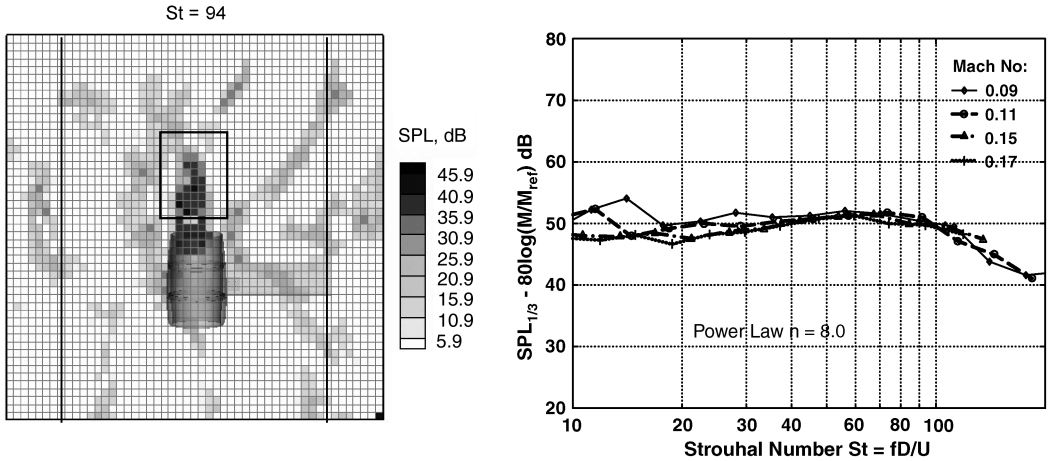

Fig. 13 Outflow-domain-based one-third-octave-band spectra scaled with Mach number to power 8.0 for 47 deg swirl-vane-angle setting; DAMAS source noise map at $St = 94$.

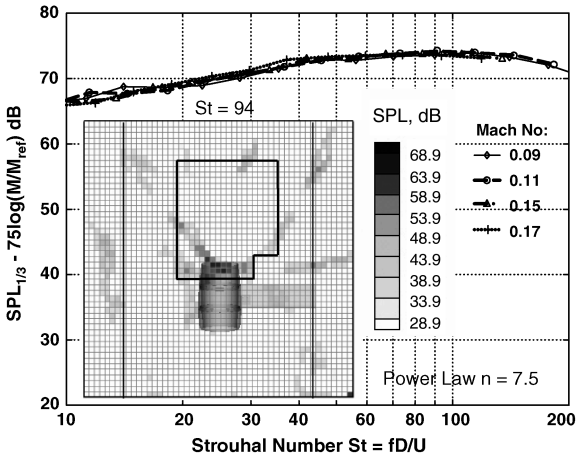

Fig. 14 Aft-region-based one-third-octave-band spectra scaled with Mach number to power 7.5 for 57 deg swirl-vane-angle setting; DAMAS source noise map at $St = 94$.

agreement for a derived power of 7.5, over the entire aft zone. The results indicate that both scattering and turbulent mixing noise are at play. Figure 14 depicts the scaled spectra and a typical DAMAS source map at a Strouhal number of 94, illustrating that the burst vortex structure close to the duct exit concentrates the noise source in that region.

In summary, three distinct acoustic features associated with stable swirling flow and vortex breakdown in the vicinity of nacelle and vane edges were identified. The results suggest that stable swirling-flow noise is governed by two distinct source mechanisms:

1) Scattering and dipole-type noise are observed to scale with the freestream Mach number to the power 6.5 for Strouhal numbers near 50 (the presence of swirl seems to alter the classic trailing-edge noise Mach number scaling law yielding exponents higher than 5).

2) The quadrupole-type turbulent mixing noise of the vortex core scales with a power of 8 for a Strouhal number near 100, similar to jet noise.

Swirling flows with vortex breakdown have substantially higher overall noise levels and appear to scale with freestream Mach number to the power of 7.5 for the entire Strouhal number range. This suggests that the vortex breakdown noise-generation process is governed by both scattering and quadrupole-type sources.

VII. Conclusions

A rigorous aeroacoustic assessment of drag-generating swirling exhaust flows was presented. The technical approach combined an in-depth aerodynamic analysis, plausibility arguments to qualitatively describe the nature of acoustic sources, and detailed quantitative acoustic measurements using a medium-aperture directional microphone array in combination with a previously established DAMAS postprocessing technique. A model-scale engine nacelle with stationary swirl vanes was designed and tested in the NASA LaRC Quiet Flow Facility at a full-scale approach Mach number of 0.17. The analysis showed that the acoustic signature is composed of quadrupole-type turbulent mixing noise of the swirling core flow and scattering and dipole-type noise from vane boundary layers and turbulent eddies of the burst vortex structure near sharp edges. Mach number scaling laws were established for both stably swirling flows and flows with vortex breakdown. For the highest stable swirl-angle setting of 47 deg, a nacelle-area-based drag coefficient of 0.83 was achieved with a full-scale overall sound pressure level of about 40 dBA at the International Civil Aviation Organization approach certification point.

Acknowledgments

This research was funded by NASA Langley Research Center, Russell Thomas contract monitor. The authors would like to thank Jack Kerrebrock and Ed Greitzer for their inspiration and insightful discussions on swirling flows. The invaluable help and support of Dan Stead, Larry Becker, Jay Moen, and Dennis Kuchta at NASA Langley Research Center is gratefully acknowledged. Special thanks go to Ronnie Geouge for his assistance with the test hardware throughout the experiments.

References

[1] Shah, P., "Novel Turbomachinery Concepts for Highly Integrated Airframe/Propulsion Systems," Ph.D. Thesis, Dept. of Mechanical Engineering, Massachusetts Inst. of Technology, Cambridge, MA, Oct. 2006.

[2] Shah, P., Mobed, D., and Spakovszky, Z., "A Novel Turbomachinery Air-Brake Concept for Quiet Aircraft," *ASME Turbo Expo 2007: Power for Land, Sea, and Air (GT2007)*, Vol. 6, Pts. A, B, ASME International, New York, 2007, pp. 1497–1510; also ASME International, Paper GT2007-27635, 2007. doi:10.1115/GT2007-27635

[3] Greitzer, E., Tan, C., and Graf, M., *Internal Flow—Concepts and Applications*, Cambridge Univ. Press, New York, 2004.

[4] Tanna, H., and Morfey, C., "Sound Radiation from Point Sources in Circular Motion," *Journal of Sound and Vibration*, Vol. 16, No. 3, 1971, pp. 337–348. doi:10.1016/0022-460X(71)90591-8

[5] Tanna, H., "On the Effect of Swirling Motion of Sources on Subsonic Jet Noise," *Journal of Sound and Vibration*, Vol. 29, No. 3, 1973, pp. 281–293. doi:10.1016/S0022-460X(73)80285-8

[6] Schwartz, I., "Swirling-Flow Jet Noise Suppressors for Aircraft Engines," AIAA Aero-Acoustics Conference, AIAA Paper 1973-1003, Seattle, WA, Oct. 1973.

[7] Lu, H., Ramsay, J., and Miller, D., "Noise of Swirling Exhaust Jets," *AIAA Journal*, Vol. 15, No. 5, May 1977, pp. 642–646. doi:10.2514/3.60673

[8] Tam, C., and Auriault, L., "Jet Mixing Noise from Fine-Scale Turbulence," *AIAA Journal*, Vol. 37, No. 2, Feb. 1999, pp. 145–153. doi:10.2514/2.691

[9] Morris, P. J., and Farassat, F., "Acoustic Analogy and Alternative Theories for Jet Noise Prediction," *AIAA Journal*, Vol. 40, No. 4, April 2002, pp. 671–680. doi:10.2514/2.1699

[10] Ffowcs Williams, J., and Hall, L., "Aerodynamic Sound Generation by Turbulent Flow in the Vicinity of a Scattering Half Plane," *Journal of Fluid Mechanics*, Vol. 40, Pt. 4, 1970, pp. 657–670. doi:10.1017/S0022112070000368

[11] Dowling, A., and Ffowcs Williams, J., *Sound and Sources of Sound*, Ellis Horwood, London, 1983.

[12] Brooks, T., Pope, S., and Marcolini, M., "Airfoil Self-Noise and Prediction," NASA Ref. Publ. 1218, July 1989.

[13] Hutcheson, F., and Brooks, T., "Measurement of Trailing Edge Noise Using Directional Array and Coherent Output Power Methods," *International Journal of Aeroacoustics*, Vol. 1, No. 4, 2002, pp. 329–354. doi:10.1260/147547202765275952

[14] Brooks, T., and Humphreys, W., Jr., "Flap Edge Aeroacoustic Measurements and Predictions," *Journal of Sound and Vibration*, Vol. 261, No. 1, 2003, pp. 31–74. doi:10.1016/S0022-460X(02)00939-2

[15] Mobed, D. D., "Experimental Aero-Acoustic Assessment of Swirling Flows for Drag Applications," M. S. Thesis, Dept. of Aeronautics and Astronautics, Massachusetts Inst. of Technology, Cambridge, MA, Feb. 2007.

[16] Brooks, T., and Humphreys, W., Jr., "A Deconvolution Approach for the Mapping of Acoustic Sources (DAMAS) Determined from Phased Microphone Arrays," *Journal of Sound and Vibration*, Vol. 294, No. 4–5, July 2006, pp. 856–879. doi:10.1016/j.jsv.2005.12.046

[17] Brooks, T., and Humphreys, W., Jr., "Three-Dimensional Application of DAMAS Methodology for Aeroacoustic Noise Source Definition," 11th AIAA/CEAS Aeroacoustics Conference, AIAA Paper 2005-2960, Monterey, CA, May 2005.

[18] Delery, J. M., "Aspects of Vortex Breakdown," *Progress in Aerospace Sciences*, Vol. 30, No. 1, 1994, pp. 1–59. doi:10.1016/0376-0421(94)90002-7

[19] Leibovich, S., "The Structure of Vortex Breakdown," *Annual Review of Fluid Mechanics*, Vol. 10, Jan. 1978, pp. 221–246. doi:10.1146/annurev.fl.10.010178.001253

M. Glauser
Associate Editor